# Identifying Potentially Risky Phases Leading to Knee Musculoskeletal Disorders during Shingle Installation Operations

Amrita Dutta[1]; Scott P. Breloff[2]; Fei Dai, M.ASCE[3]; Erik W. Sinsel[4]; Christopher M. Warren[5]; and John Z. Wu[6]

**Abstract:** Repeated and prolonged awkward kneeling can result in musculoskeletal disorders (MSD) in construction roofers. However, a task-specific risk assessment for roofers' knee injuries is still missing in the literature. This study identified a ranking-based ergonomic method for suggesting potentially risky phases that may increase knee MSD risk during shingle installation operations. On a slope-adjustable wooden platform in a laboratory setting, nine subjects performed shingle installations that included seven phases: (1) reaching for shingles, (2) placing shingles, (3) grabbing nail gun, (4) moving to first nailing position, (5) nailing shingles, (6) replacing nail gun, and (7) returning to upright position. Flexion, abduction, adduction, and internal and external knee rotations were measured to assess relative risks of these phases by ranking them with a scoring model. The ranking results revealed that the phases of placing shingles and nailing shingles lead to the most knee MSD risk exposure, and awkward flexion, abduction, and adduction involved in these phases can significantly contribute to the potential knee MSD risk measurement. By using the ranking-based method, this study suggested that certain phases of the shingle installation process may increase knee MSD risk, which is useful for developing effective interventions to reduce knee injury risk exposures from roof shingle installation. **DOI: 10.1061/(ASCE)CO.1943-7862.0001783.** 

**Author keywords:** Experimental study; Construction ergonomics; Risk assessment; Construction safety.

## Introduction

Shingle installation is a prolonged, repetitive, and awkward task that residential roofers commonly preform on the jobsite. Shingle installation involves awkward crawling, stooping, or kneeling postures and repetitive motions that result in roofers' knee musculoskeletal disorders (MSD) including chronic knee pain, knee joint irritation (i.e., bursitis), and osteoarthritis (Dulay et al. 2015). As roofers spend more than 75% of their total working time restricted to awkward postures and repetitive motions in a sloped roof setting, they suffer from a high incidence rate of MSD (CPWR 2018). It has been shown that awkward knee postures and repetitive motions are associated with knee MSD (Hofer et al. 2011). Nevertheless, it is still unknown which phases of the shingle installation operation might yield the most awkward postures and repetitive motions that result in potentially the greatest knee MSD risk on slanted roof surfaces. A detailed ranking of the typical kneeling shingle installation phases based on the awkward postures and repetitive rotations can provide insights into the association of these phases with knee MSD risk development. Although ranking-based methods were applied to study risks in construction associated with schedule delays (Bagaya and Song 2016), life-cycle of green buildings (Qin et al. 2016), and highway construction projects (El-Sayegh and Mansour 2015), they are yet to be applied in investigations of work-related MSD risks. It would be helpful to rank the phases in a sloped kneeling shingle installation process based on the MSD risk caused by awkward postures and repetitive motions. Such a ranking could reveal the shingle installation phases that pose the greatest risk of knee MSD, improving the focus and development of new intervention methods.

## Background

### Prevalence of Knee Injuries among Roofers

According to the "Nonfatal Occupational Injuries and Illnesses" report of 2016, 38% of the total injuries involving lower extremities were located in the knees (BLS 2017). According to Wang et al. (2015), roofers' MSD rate is 30% higher than the average MSD incident rate reported for all construction trades. In the state of Washington, the insurance premium composite base rate for roofers is the highest ($7.03) among all building construction trades (Washington State Department of Labor & Industries 2018). It is apparent that there is a pressing need to alleviate the ergonomic injuries

[1]Graduate Research Assistant, Dept. of Civil and Environmental Engineering, West Virginia Univ., P.O. Box 6103, Morgantown, WV 26506. Email: amdutta@mix.wvu.edu

[2]Biomedical Research Engineer, National Institute for Occupational Safety and Health, 1095 Willowdale Rd., Morgantown, WV 26505. Email: sbreloff@cdc.gov

[3]Associate Professor, Dept. of Civil and Environmental Engineering, West Virginia Univ., P.O. Box 6103, Morgantown, WV 26506 (corresponding author). ORCID: https://orcid.org/0000-0002-8868-2821. Email: fei.dai@mail.wvu.edu

[4]Computer Scientist, National Institute for Occupational Safety and Health, 1095 Willowdale Rd., Morgantown, WV 26505. Email: ESinsel@cdc.gov

[5]Mechanical Engineer, National Institute for Occupational Safety and Health, 1095 Willowdale Rd., Morgantown, WV 26505. Email: cpw4@cdc.gov

[6]Senior Research Biomechanical Engineer, National Institute for Occupational Safety and Health, 1095 Willowdale Rd., Morgantown, WV 26505. Email: ozw8@cdc.gov

Note. This manuscript was submitted on May 30, 2019; approved on August 12, 2019; published online on December 31, 2019. Discussion period open until May 31, 2020; separate discussions must be submitted for individual papers. This paper is part of the ***Journal of Construction Engineering and Management***, © ASCE, ISSN 0733-9364.

and to develop interventions for reducing knee MSD among construction roofers.

### State of Practice in Ergonomics to Prevent Kneeling-Related Injuries among Roofers

To protect the roofers from knee MSD, some generic solutions suggested in the existing literature include the use of powered mechanical caulk and seam welding equipment and the wearing of knee pads while kneeling and installing new roofs (Spielholz et al. 2006). To reduce the risk of resulting MSD among construction workers, safety and health organizations have recommended general ergonomic practices and guidelines as well. For example, a booklet titled *Simple Solutions: Ergonomics for Construction Workers* published by the National Institute for Occupational Safety and Health (NIOSH) suggests using knee supporting devices such as kneeling creeper and knee pads that may prevent additional stress on knees in construction work that requires kneeling (Albers and Estill 2007). Similar protective devices such as knee pads and power stretchers for kneeling are suggested in web-based training tools (eTools) promoted by OSHA (2019). However, these protective measures are generic; and even if they can prevent knee injuries, they are designed for work on flat surfaces. Guidelines are still lacking for tasks performed on slanted rooftops for knee injury prevention for roofers.

### State of Ergonomics Research on MSD among Roofers

Previous ergonomic studies mainly focused on severity, prevalence, and causes of ergonomic injuries among roofers. In a survey study, motion/position and overexertion were revealed as the two most prevalent sources of nonfatal injuries to roofers (Fredericks et al. 2005). A laboratory assessment done by Choi (2008) found that roofers experience greater pain in their lower extremities during shingle installation on sloped roof surfaces than roofers on flat surfaces. Roofers' MSD has been identified as a possible cause of reduced physical functioning and disability in workplaces (Welch et al. 2010). In a pilot study conducted by Lee et al. (2017), the feasibility of wearable sensors, such as activity trackers and physiological monitors, were assessed in facilitating data collection about roofers' heart rate, energy expenditure, metabolic equivalents, and sleep efficiency. Wang et al. (2017) examined the work-related risk factors of roof slope, working technique, working pace, and posture to the development of low back disorders among roofers and found significant association of these factors to cause low back disorders among roofers. A similar study assessed the effects of roof slope and kneeling posture as two potential risk factors to knee MSD development in a sloped kneeling shingle installation task (Breloff et al. 2019a). Lower extremity kinematics of roofers at cross-slope roof walking were investigated by Breloff et al. (2019b), leading to establishment of their associations to MSD.

## Problem Statement and Research Objective

Based on this review, in-depth insights into work-specific risk exposures for roofers' knees during shingle installation are still lacking. As roofers frequently perform shingle installation, the required constant awkward and extreme kneeling posture causes bending of their knees, sometimes exceeding their normal range of motion, for a prolonged time. It has been proven that awkward knee rotations and repetitive motions can lead to knee MSD (Hofer et al. 2011). A ranking of the kneeling shingle installation phases based on MSD risk caused by awkward knee rotations and repetitive motions might suggest those phases that potentially lead to the greatest knee MSD risk. These findings could be vital to the development of targeted interventions to prevent knee MSD of roofers. However, such a ranking is still missing. Therefore, the objective of this study is to identify a ranking-based ergonomic method for suggesting the potential risky phases in terms of awkward knee rotations and repetitive motions during shingle installation operations on slanted surfaces.

## Methodology

Fig. 1 shows an overview of the methodology, according to which time-series knee kinematics data, in terms of five knee rotation angles—flexion, abduction, adduction, and internal and external rotations, were used to compute 15 risk indicators for each phase of the shingle installation process. By using these risk indicators, the phases were then ranked by all five and individual knee rotations, respectively. In ranking phases by all five knee rotations, 15 total risk indicators were combined to generate a risk score for each phase, which was considered as the measure of the risk to rank the relative risk of the phases based on awkward and extreme knee rotations. In ranking phases by individual knee rotation, only 3 risk indicators associated with each individual knee rotation (e.g., flexion) were combined to generate a risk score of each phase for risk ranking. Based on the resulting rankings, lastly, the relative contribution of each knee rotation to the knee MSD risk measurement was analyzed by correlating the rankings generated from each knee rotation with the ranking generated from all knee rotations. The following presents the methodology in detail. It first defines the shingle installation phases. This is followed by selection of the risk indicators. Next, the steps involved in the workflow of this methodology are elaborated.

### Shingle Installation Phases Definition

In a typical shingle installation process, roofers place and install shingles by nailing with a pneumatic nail-gun. Specifically, roofers start this process by reaching for shingles first and then placing them, facing forward, on the roof surface. Next, they grab the nail gun from aside and become ready to start nailing shingles. After that, they nail shingles side by side. They finish the shingle installation process by replacing the nail gun and returning to their initial upright position. As a result, seven phases were defined in this study (Fig. 2), and the kinematics data were subsequently segmented for analysis according to these phase definitions.

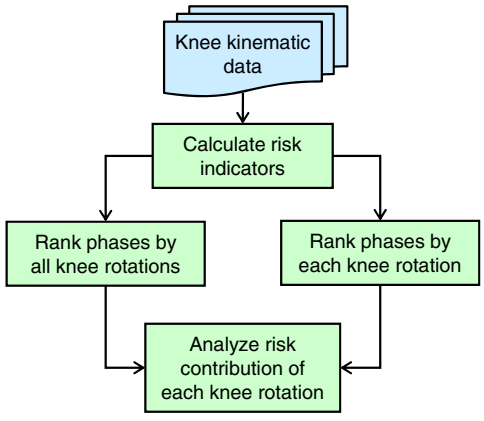


**Fig. 1.** Methodology overview.

| Phase | Task performed | Illustration |
|---|---|---|
| Phase 1 | Reaching for shingles | 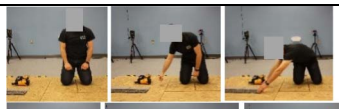 |
| Phase 2 | Placing the shingles |  |
| Phase 3 | Grabbing the nail gun | 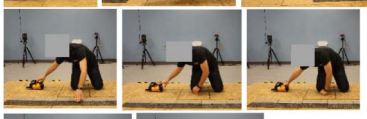 |
| Phase 4 | Moving to first nailing position |  |
| Phase 5 | Nailing shingles |  |
| Phase 6 | Replacing the nail gun |  |
| Phase 7 | Returning to upright position |  |

**Fig. 2.** Seven phases of shingle installation trial defined.

### *Risk Indicator Selection*

During the shingle installation process, the repeated deep kneeling posture encountered by the roofers increases the risk of knee MSD due to the extreme and awkward position of the knee joint. Repeated and high contact stress at the knee joint contributes to knee MSD, such as knee osteoarthritis and damage of articular cartilage of the knee joint (Kajaks and Costigan 2015). Kneeling with a deep-flexed position (beyond 90°) produces large forces and moments that may result in high-contact stress in the knee joint surface (Nagura et al. 2002). A significant increase (by over 80%) in the knee joint contact stress was observed with an increase in knee flexion from 15.5° to 90° (Thambyah et al. 2005). These findings represent a strong association between knee rotations and knee joint contact stress that can relate to knee MSD. As knee rotations undergo larger awkward postures during shingle installation and impose more awkward positions on the knee joint, thereby increasing knee joint contact force, knee MSD risk is considered to increase. Awkward knee posture is considered as a deep flexed position of the knee (>90°) accompanied by medial and lateral rotations that cause an increased amount of joint contact stress. Hence, this study defines risk as an increase in awkward knee rotations that may increase the knee joint contact stress.

To assess the impact of awkward kneeling postures and repetitive motions at different kneeling shingling installation phases, five knee rotations—flexion (about the medio-lateral axis), abduction and adduction (about the anterior-posterior axis), and internal and external rotations (about the longitudinal axis) were measured (Fig. 3). Deep flexion activities produce large force and moment on the knee joint (Nagura et al. 2006). High knee adduction and abduction impose stress on the knee joint and increase the risk of developing knee osteoarthritis (Barrios et al. 2010). Internal and

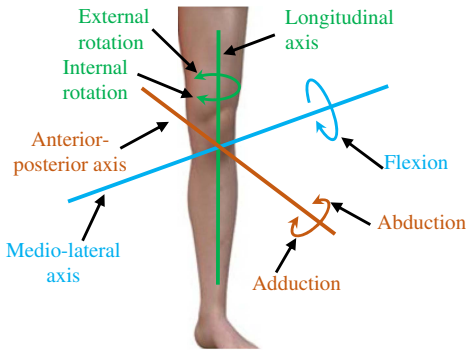


**Fig. 3.** Five knee rotation angles.

external rotations of the tibia relative to the femur place additional stress on the knee joint's ligaments (Coplan 1989; Hofer et al. 2011). As the shingle installation is a dynamic process, three metrics, including maximum, cumulative, and average measurements of these five knee rotations, were extracted from the time series kinematic data as risk indicators. These metrics have been found to have significant associations with the MSD risk to upper and lower limbs (Gyemi et al. 2016; Hatfield et al. 2015; McClellan et al. 2009; Zampporri and Aguinaldo 2017). In a particular trial, the maximum knee rotation value for a phase refers to the peak knee rotation angle within that phase. As the extreme and awkward postures are associated with MSD, it is advantageous to evaluate the maximum knee rotation that could relate to the extreme rotation of knees due to forceful exertion in the shingle installation operation. Knee MSD risks can increase when roofers work in an awkward

posture for a long period of time without adequate recovery time. The cumulative knee rotation value is the summation of the knee rotation angles across that phase. It represents the risk due to maintaining an awkward knee rotation angle over time. The average knee rotation value for a phase represents the mean knee rotation within that phase. It accounts for the risk due to knee repetitive motions. If the roofers perform the same task that involves rotations in their knees repeating every few seconds even under their tolerance limit, they can still develop knee MSD. Therefore, these metrics (maximum, cumulative, and average measurements) of the five knee rotations (flexion, abduction, adduction, and internal and external rotations) were selected, resulting in 15 risk indicators at each phase.

### Workflow Details

#### Calculating Risk Indicators

The calculation of the risk indicators for each phase follows the procedures described subsequently. Because the calculation procedure for each knee rotation is the same, the flexion angle calculation is shown as an example.

Let the flexion angle of the certain knee (i.e., left or right) observed for subject $x$ at trial $t$, phase $p$, and time $i$ be represented as $F_{x,t,p,i}$.

Then, the maximum flexion for subject $x$ at trial $t$, and phase $p$ will be

$$F^{max}_{x,t,p} = \max_i(F_{x,t,p,i}) \tag{1}$$

The cumulative flexion for subject $x$ at trial $t$, and phase $p$ will be

$$F^{cum}_{x,t,p} = \sum_i F_{x,t,p,i} \tag{2}$$

The average flexion for subject $x$ at trial $t$, and phase $p$ will be

$$F^{avg}_{x,t,p} = \text{avg}_i(F_{x,t,p,i}) \tag{3}$$

These values are then averaged over all subjects and trials to compute risk indicators. So, by using Eqs. (1)–(3), three risk indicators associated with the flexion at phase $p$ will be derived as

$$\{F^{max}_p, F^{cum}_p, F^{avg}_p\} = \{\text{avg}_x[\text{avg}_t(F^{max}_{x,t,p})], \text{avg}_x[\text{avg}_t(F^{cum}_{x,t,p})], \text{avg}_x[\text{avg}_t(F^{avg}_{x,t,p})]\} \tag{4}$$

Similarly, these equations were used to compute the risk indictors at phase $p$ for the abduction, adduction, internal, and external knee rotations. Given $p \in [1, 7]$, a total number of 105 risk indictors were obtained for all seven phases. Both the left and right knees' risk indictors were computed.

#### Ranking Phases by All Knee Rotations

The seven shingle installation phases were first ranked considering the set of all knee rotations. To this end, the 15 risk indicators—maximum, cumulative, and average angles of all five knee rotations were combined by applying a scoring model to generate a risk score for each phase. The resulting risk scores were then compared for ranking the phases. The phase that had the highest score was considered potentially riskiest for knee MSD. The resulting ranking is referred to as "multi-angle-based ranking" in this study, because it accounts for the contributions of all five knee rotations to the measurement of the risk scores, and the ranking represents the knee MSD risk associated with multiple awkward knee rotations. Due to the dynamic nature of the shingling process—the multi-angle-based rankings were computed separately for the left and right knees.

#### Ranking Phases by Individual Knee Rotation

The seven phases were then ranked based on individual knee rotations to help understand the impact of each knee rotation on the imposed risks. For this, instead of using the 15 risk indicators, only three risk indicators (i.e., maximum, cumulative, and average angles) of certain knee rotations were considered. For example, to assess the risk due to flexion, only the three risk indicators of the flexion rotation were used to generate the flexion-based phase ranks by applying the scoring model. These rankings computed based on individual knee rotations were referred to as "single-angle-based rankings," becasuse they accounted for the contribution of individual knee rotations to the measurement of the risk scores and represented the knee MSD risk associated with that individual knee rotation of interest. A total of five single-angle-based rankings were generated for the seven phases. Similar to the multi-angle-based ranking, the single-angle-based rankings were separately analyzed for each knee.

#### Assessing the Relative Contribution of Each Knee Rotation to Potential Knee MSD Risk Measurement

To analyze which angle significantly contributed to the knee MSD risk measurement, associations between the multi-angle-based ranking and the five single-angle-based rankings of the phases were further analyzed by computing Spearman's rank correlation coefficient with the equation $1 - 6\sum d^2/(N^3 - N)$, where $d$ is the difference in rankings; and $N$ is the number of variables (phases = 7) (Rosso 1997). The Spearman's rank correlation coefficient indicates the strength of association between two rankings. The higher the value (approaching 1), the stronger the association between rankings. The rotation angle with the highest coefficient value is deemed to have the strongest influence on the multi-angle-based ranking that relates to the potential knee MSD risk measurement associated with multiple knee rotations.

## Implementation and Results

### Participants

This study included nine male participants [26.1 years (5.6 years), 180.2 cm (6.1 cm), and 99.7 kg (27.6 kg)] without any prior roofing experience in the experiment. No participant was suffering from any known MSD or neurological diseases. The research protocol was approved by both the Institutional Review Boards (IRB) of the National Institute for Occupational Safety and Health and West Virginia University.

### Instruments

An optical motion capture system equipped with 14 MX cameras (VICON, Oxford, UK) was used to collect the segment endpoint data of the participants. Forty-two retroreflective markers for motion capture were placed bilaterally on the lower extremities of the participants, including feet, heels, toes, ankles, shanks, knee joints, thighs, and hip joints, as illustrated in Fig. 4. The collected three-dimensional (3D) coordinates of these markers were used to calculate knee angles. The kinematic data were recorded at 100 Hz.

A $1.2 \times 1.6$ m custom-made adjustable wood platform was used to mimic the roof surface for shingle installation. A battery-powered lift would raise the roof platform, which could be adjusted

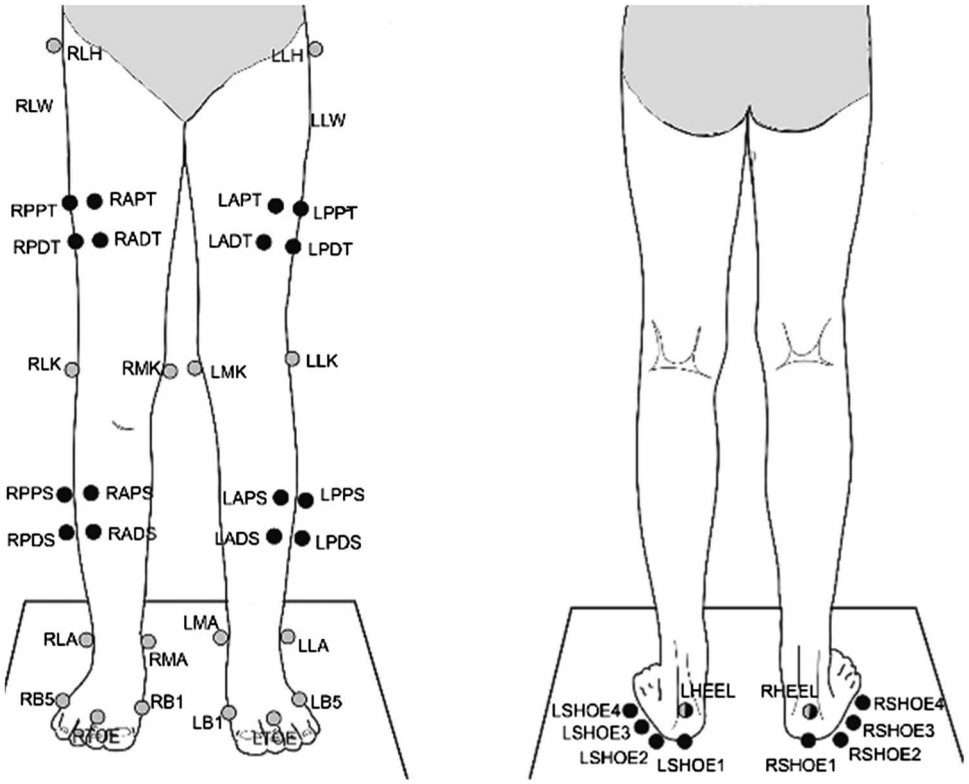


**Fig. 4.** Marker positions.

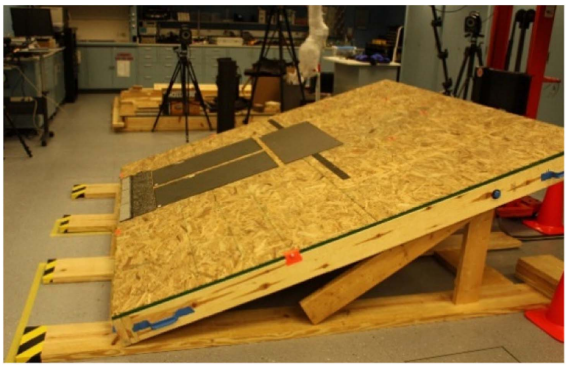

**Fig. 5.** Wooden platform for roofing simulation.

to a slope angle ranging from 0° to over 30° by two sets of wooden legs (Fig. 5).

### Procedure

The experiment was conducted in the biomechanics laboratory at NIOSH. Motion markers for kinematic calibration and data collection were placed on participants upon their arrival at the lab. Participants were in a deep kneeling posture on the roof simulator prior to the start of data collection. When instructed to begin, participants first reached for and placed two shingles in front of them. Then they picked up the nail gun from their right side and mimicked affixing six nails (three in each) into the two shingles side by side on the roof simulator, starting on the left and moving to the right of the shingle. Once finished, the participants replaced the nail gun and returned to their resting/starting position. To sum, the participants performed the seven phases of the shingle installation task as one continuous activity. Each participant performed the simulated shingle installation task on the roof simulator at three slope angles—0°, 15°, and 30°. At each slope angle, the task was performed five times by each participant. This resulted in data from 45 trials (5 trials × 9 participants) at each slope angle.

### Data Processing

By using the coordinates of the markers captured, the five knee rotations were computed in Visual 3D version 6 with the method provided by Robertson et al. (2013). These knee rotation data were collected at a rate of 100 data points per second during each trial, resulting in a huge set of data points. From these data points, the maximum, cumulative, and average of the five knee rotations for each phase were computed for a certain knee (left/right) on each slope. This way, for a certain knee at each slope, 315 (9 participants × 5 trials × 7 phases) data points of maximum, cumulative, and average of the five knee rotations were obtained, respectively. These knee rotations were then used to formulate the risk indicators necessary for the subsequent analysis.

### Risk Indicators

Tables 1 and 2 present the 15 risk indicators—the maximum, cumulative, and average of the five rotations averaged over all subjects and trials—across seven phases, on three slopes for the left and right knees, respectively.

### Multi-Angle-Based Ranking

This study implemented two types of scoring models—an "aggregation-based scoring model" and a "multiplication scoring model" for the multi-angle-based ranking, both of which have been proven

**Table 1.** Risk indicators computed for left knee

| Indicators | Phases | Slopes 0° | 15° | 30° |
|---|---|---|---|---|
| Maximum flexion (°) | 1 | 137.0 | 133.6 | 137.6 |
| | 2 | 135.1 | 130.8 | 128.4 |
| | 3 | 133.7 | 128.7 | 120.3 |
| | 4 | 135.2 | 129.6 | 122.1 |
| | 5 | 131.9 | 123.5 | 117.5 |
| | 6 | 132.0 | 127.5 | 126.9 |
| | 7 | 137.4 | 133.1 | 137.0 |
| Maximum abduction (°) | 1 | 9.6 | 8.5 | 9.5 |
| | 2 | 7.2 | 7.9 | 10.0 |
| | 3 | 7.6 | 8.7 | 7.8 |
| | 4 | 7.7 | 8.5 | 11.9 |
| | 5 | 8.1 | 8.6 | 12.3 |
| | 6 | 8.3 | 8.3 | 8.0 |
| | 7 | 10.8 | 8.3 | 9.5 |
| Maximum adduction (°) | 1 | −5.2 | −3.1 | −4.8 |
| | 2 | −6.1 | −3.3 | −4.7 |
| | 3 | −5.1 | −2.8 | −4.0 |
| | 4 | −4.4 | −3.0 | −4.2 |
| | 5 | −8.2 | −5.5 | −4.3 |
| | 6 | −8.5 | −5.4 | −4.4 |
| | 7 | −5.4 | −3.7 | −4.8 |
| Maximum internal rotation (°) | 1 | 5.1 | 10.4 | 10.4 |
| | 2 | 5.2 | 10.4 | 9.5 |
| | 3 | 4.7 | 8.4 | 8.1 |
| | 4 | 4.4 | 8.6 | 8.5 |
| | 5 | 5.7 | 7.4 | 8.3 |
| | 6 | 5.8 | 7.4 | 8.3 |
| | 7 | 5.4 | 10.2 | 10.0 |
| Maximum external rotation (°) | 1 | −8.8 | −8.5 | −7.3 |
| | 2 | −8.9 | −9.2 | −9.5 |
| | 3 | −7.8 | −9.9 | −8.1 |
| | 4 | −8.6 | −9.7 | −8.8 |
| | 5 | −10.0 | −8.8 | −8.7 |
| | 6 | −7.7 | −7.9 | −7.8 |
| | 7 | −9.4 | −8.4 | −7.9 |
| Cumulative flexion (°) | 1 | 22,688.0 | 18,979.0 | 20,714.0 |
| | 2 | 58,899.0 | 52,254.0 | 61,009.0 |
| | 3 | 9,249.0 | 9,389.0 | 8,896.0 |
| | 4 | 16,074.0 | 15,015.0 | 15,412.0 |
| | 5 | 37,125.0 | 32,926.0 | 31,460.0 |
| | 6 | 13,553.0 | 13,686.0 | 12,243.0 |
| | 7 | 20,461.0 | 20,789.0 | 19,589.0 |
| Cumulative abduction (°) | 1 | 1,348.0 | 1,113.0 | 1,179.0 |
| | 2 | 2,453.0 | 2,687.0 | 3,342.0 |
| | 3 | 509.0 | 667.0 | 500.0 |
| | 4 | 701.0 | 832.0 | 1,133.0 |
| | 5 | 1,731.0 | 1,900.0 | 2,410.0 |
| | 6 | 752.0 | 774.0 | 689.0 |
| | 7 | 1,267.0 | 1,136.0 | 1,092.0 |
| Cumulative adduction (°) | 1 | −623.0 | −275.0 | −509.0 |
| | 2 | −1,618.0 | −720.0 | −1,202.0 |
| | 3 | −263.0 | −170.0 | −265.0 |
| | 4 | −337.0 | −168.0 | −409.0 |
| | 5 | −1,223.0 | −712.0 | −699.0 |
| | 6 | −664.0 | −424.0 | −297.0 |
| | 7 | −511.0 | −365.0 | −472.0 |
| Cumulative internal rotation (°) | 1 | 560.0 | 1,228.0 | 1,350.0 |
| | 2 | 1,155.0 | 3,110.0 | 3,265.0 |
| | 3 | 227.0 | 546.0 | 552.0 |
| | 4 | 311.0 | 742.0 | 827.0 |
| | 5 | 967.0 | 1,240.0 | 1,726.0 |
| | 6 | 438.0 | 555.0 | 537.0 |
| | 7 | 412.0 | 1,165.0 | 1,170.0 |
| Cumulative external rotation (°) | 1 | −985.0 | −865.0 | −579.0 |
| | 2 | −2,022.0 | −2,605.0 | −3,034.0 |
| | 3 | −436.0 | −648.0 | −503.0 |
| | 4 | −639.0 | −778.0 | −832.0 |
| | 5 | −1,616.0 | −1,615.0 | −1,743.0 |
| | 6 | −564.0 | −765.0 | −682.0 |
| | 7 | −885.0 | −935.0 | −716.0 |
| Average flexion (°) | 1 | 127.7 | 130.5 | 133.9 |
| | 2 | 128.8 | 126.9 | 118.3 |
| | 3 | 131.7 | 126.5 | 116.8 |
| | 4 | 131.9 | 124.9 | 118.6 |
| | 5 | 126.1 | 117.3 | 112.9 |
| | 6 | 125.9 | 120.1 | 117.8 |
| | 7 | 130.5 | 130.1 | 132.0 |
| Average abduction (°) | 1 | 7.6 | 7.5 | 7.9 |
| | 2 | 5.6 | 6.1 | 6.5 |
| | 3 | 6.8 | 8.2 | 6.9 |
| | 4 | 5.9 | 6.3 | 8.4 |
| | 5 | 6.0 | 6.2 | 8.6 |
| | 6 | 7.7 | 7.4 | 6.8 |
| | 7 | 7.9 | 6.5 | 7.6 |
| Average adduction (°) | 1 | −3.2 | −1.9 | −2.9 |
| | 2 | −3.9 | −1.7 | −1.9 |
| | 3 | −4.4 | −2.3 | −3.0 |
| | 4 | −2.9 | −1.4 | −3.1 |
| | 5 | −4.3 | −2.4 | −2.3 |
| | 6 | −5.6 | −3.5 | −2.8 |
| | 7 | −3.2 | −2.4 | −3.4 |
| Average internal rotation (°) | 1 | 3.2 | 8.8 | 8.2 |
| | 2 | 2.5 | 7.6 | 6.0 |
| | 3 | 3.4 | 7.6 | 7.2 |
| | 4 | 2.5 | 5.9 | 6.1 |
| | 5 | 3.3 | 4.1 | 6.4 |
| | 6 | 3.7 | 4.6 | 5.7 |
| | 7 | 2.8 | 7.9 | 7.9 |
| Average external rotation (°) | 1 | −5.6 | −6.5 | −4.6 |
| | 2 | −5.3 | −6.9 | −6.2 |
| | 3 | −6.3 | −8.9 | −6.9 |
| | 4 | −5.8 | −7.2 | −7.0 |
| | 5 | −6.0 | −6.5 | −6.5 |
| | 6 | −5.9 | −6.2 | −6.5 |
| | 7 | −5.7 | −6.0 | −5.3 |

to be useful in ranking tasks with multiple criteria (El-Sayegh and Mansour 2015; Tofallis 2012, 2014).

Typically, the aggregation-based scoring model includes three steps: (1) data normalization; (2) indicator weighing; and (3) weighted indictor aggregation; to generate an overall risk score for ranking. For data normalization, the following methods were tested for each risk indicator in this study:

- Dividing by maximum: It converted the value of a risk indicator (e.g., Maximum flexion) for a certain phase as proportion of the maximum (e.g., maximum of Maximum flexion) among the seven phases as

$$Y = \frac{X}{X_{max}} \tag{5}$$

- Dividing by sum: It converted the value of a risk indictor (e.g., Maximum flexion) for a certain phase as proportion of

**Table 2.** Risk indicators computed for right knee

| Indicators | Phases | Slopes 0° | Slopes 15° | Slopes 30° |
|---|---|---|---|---|
| Maximum flexion (°) | 1 | 138.0 | 138.0 | 139.3 |
| | 2 | 135.0 | 135.0 | 130.0 |
| | 3 | 133.0 | 132.0 | 121.0 |
| | 4 | 134.0 | 133.0 | 122.0 |
| | 5 | 131.0 | 126.0 | 117.0 |
| | 6 | 132.0 | 131.0 | 128.0 |
| | 7 | 137.0 | 137.5 | 139.0 |
| Maximum abduction (°) | 1 | 9.2 | 9.2 | 8.0 |
| | 2 | 7.1 | 6.3 | 6.0 |
| | 3 | 5.5 | 5.3 | 5.5 |
| | 4 | 5.8 | 4.9 | 5.9 |
| | 5 | 6.0 | 6.4 | 6.7 |
| | 6 | 5.7 | 6.4 | 6.8 |
| | 7 | 8.8 | 8.0 | 7.9 |
| Maximum adduction (°) | 1 | −5.7 | −62.0 | −7.0 |
| | 2 | −8.0 | −6.8 | −7.5 |
| | 3 | −6.8 | −6.6 | −4.0 |
| | 4 | −8.9 | −6.5 | −6.8 |
| | 5 | −8.8 | −6.9 | −7.0 |
| | 6 | −5.9 | −6.5 | −5.8 |
| | 7 | −5.5 | −6.9 | −6.9 |
| Maximum internal rotation (°) | 1 | 10.0 | 13.1 | 14.4 |
| | 2 | 11.0 | 11.6 | 11.8 |
| | 3 | 9.9 | 10.0 | 12.6 |
| | 4 | 10.7 | 11.7 | 12.2 |
| | 5 | 9.4 | 11.0 | 12.4 |
| | 6 | 9.6 | 10.0 | 12.0 |
| | 7 | 10.4 | 13.0 | 14.4 |
| Maximum external rotation (°) | 1 | −9.9 | −10.1 | −8.4 |
| | 2 | −6.0 | −6.4 | −6.9 |
| | 3 | −4.7 | −5.4 | −6.7 |
| | 4 | −4.9 | −6.0 | −6.4 |
| | 5 | −7.9 | −7.3 | −9.7 |
| | 6 | −7.3 | −7.2 | −11.0 |
| | 7 | −9.1 | −9.9 | −7.1 |
| Cumulative flexion (°) | 1 | 23,509.0 | 19,630.0 | 20,111.0 |
| | 2 | 62,190.0 | 53,776.0 | 61,015.0 |
| | 3 | 9,269.0 | 9,689.0 | 8,866.0 |
| | 4 | 16,149.0 | 15,299.0 | 15,241.0 |
| | 5 | 37,608.0 | 33,956.0 | 31,075.0 |
| | 6 | 13,841.0 | 14,126.0 | 12,210.0 |
| | 7 | 20,284.0 | 21,434.0 | 18,355.0 |
| Cumulative abduction (°) | 1 | 1,245.0 | 1,185.1 | 924.0 |
| | 2 | 1,782.0 | 1,946.0 | 1,822.0 |
| | 3 | 295.0 | 374.0 | 341.0 |
| | 4 | 446.0 | 407.0 | 521.0 |
| | 5 | 834.0 | 1,091.0 | 1,103.0 |
| | 6 | 415.0 | 485.0 | 528.0 |
| | 7 | 925.0 | 1,071.0 | 896.0 |
| Cumulative adduction (°) | 1 | −598.0 | −724.0 | −729.0 |
| | 2 | −2,935.0 | −1,999.0 | −2,227.0 |
| | 3 | −405.0 | −429.0 | −270.0 |
| | 4 | −858.0 | −583.0 | −504.0 |
| | 5 | −1,787.0 | −1,215.0 | −1,089.0 |
| | 6 | −446.0 | −572.0 | −351.0 |
| | 7 | −481.0 | −800.0 | −641.0 |
| Cumulative internal rotation (°) | 1 | 1,299.0 | 1,517.0 | 1,771.0 |
| | 2 | 4,120.0 | 3,947.0 | 4,870.0 |
| | 3 | 585.0 | 660.0 | 849.0 |
| | 4 | 1,071.0 | 1,138.0 | 1,434.0 |
| | 5 | 1,979.0 | 2,400.0 | 2,843.0 |
| | 6 | 834.0 | 728.0 | 897.0 |
| | 7 | 1,053.0 | 1,560.0 | 1,453.0 |
| Cumulative external rotation (°) | 1 | −1,506.0 | −1,285.0 | −1,000.0 |
| | 2 | −1,526.0 | −1,740.0 | −1,792.0 |
| | 3 | −258.0 | −352.0 | −419.0 |
| | 4 | −428.0 | −414.0 | −562.0 |
| | 5 | −1,273.0 | −1,165.0 | −1,806.0 |
| | 6 | −567.0 | −500.0 | −840.0 |
| | 7 | −1,033.0 | −1,260.0 | −719.0 |
| Average flexion (°) | 1 | 131.8 | 134.3 | 130.7 |
| | 2 | 130.2 | 130.3 | 118.1 |
| | 3 | 131.8 | 130.5 | 116.4 |
| | 4 | 129.5 | 126.9 | 117.1 |
| | 5 | 125.1 | 120.3 | 110.9 |
| | 6 | 128.3 | 124.0 | 116.4 |
| | 7 | 129.3 | 133.9 | 124.9 |
| Average abduction (°) | 1 | 6.6 | 7.6 | 5.5 |
| | 2 | 4.3 | 4.4 | 3.5 |
| | 3 | 4.6 | 4.7 | 4.5 |
| | 4 | 4.1 | 3.2 | 3.9 |
| | 5 | 3.2 | 3.6 | 4.1 |
| | 6 | 4.3 | 4.6 | 5.1 |
| | 7 | 5.8 | 5.9 | 5.8 |
| Average adduction (°) | 1 | −3.6 | −5.2 | −4.9 |
| | 2 | −6.0 | −5.1 | −3.7 |
| | 3 | −5.8 | −6.0 | −3.1 |
| | 4 | −6.7 | −5.1 | −3.9 |
| | 5 | −5.8 | −4.6 | −3.8 |
| | 6 | −4.2 | −5.0 | −3.3 |
| | 7 | −3.2 | −5.5 | −4.7 |
| Average internal rotation (°) | 1 | 7.5 | 10.7 | 11.5 |
| | 2 | 8.1 | 9.1 | 8.1 |
| | 3 | 8.2 | 8.9 | 10.6 |
| | 4 | 8.0 | 8.8 | 10.2 |
| | 5 | 6.2 | 7.6 | 9.8 |
| | 6 | 7.2 | 6.7 | 8.7 |
| | 7 | 7.1 | 10.6 | 10.7 |
| Average external rotation (°) | 1 | −8.0 | −8.9 | −6.1 |
| | 2 | −3.5 | −4.4 | −4.1 |
| | 3 | −3.8 | −4.3 | −5.7 |
| | 4 | −3.6 | −3.8 | −4.8 |
| | 5 | −4.6 | −4.8 | −7.1 |
| | 6 | −5.7 | −4.9 | −8.7 |
| | 7 | −6.2 | −6.7 | −4.8 |

the sum (e.g., sum of Maximum flexion) across the seven phases as

$$Y = \frac{X}{\sum X} \tag{6}$$

- Range normalization: It scaled the value of a risk indicator for a certain phase to [0, 1] in regard to the maximum and minimum values of the risk indicator among the seven phases as

$$Y = \frac{X - X_{min}}{X_{max} - X_{min}} \tag{7}$$

where $X$ = value of a risk indicator for a certain phase; $\sum X$ = sum of the values of that risk indictor across all the seven phases; $X_{max}$ and $X_{min}$ = highest and lowest values of that risk indicator among the seven phases, respectively; and $Y$ = normalized value of $X$.

After normalization, weights were assigned to each risk indicator. Because no existing literature reveals the relative contribution of each knee rotation to the knee MSD risk measurement, and because all five knee rotations observed in this study were biomechanically responsible for causing knee MSD, this study assumed that all risk indicators had equal contributions to the knee injury risk and, hence, were assigned equal weights. Finally, all weighted indicators were summed to yield an overall risk score for each phase by

$$\text{Risk Score (Aggregation-based)} = w_1Y_1 + w_2Y_2 + w_3Y_3 + \cdots + w_nY_n \quad (8)$$

where $Y_i$ $(i = 1, 2, \ldots n)$ = normalized value of a risk indicator for a phase; and $w_i$ $(i = 1, 2, \ldots n)$ = weight assigned to each indicator.

Alternatively, the multiplication scoring model does not require normalization. The risk score of a phase for a set of risk indicators was calculated by

$$\text{Risk Score (Multiplication)} = X_1^{W_1} X_2^{W_2} X_3^{W_3} \ldots X_n^{W_n} \quad (9)$$

where $X_i$ $(i = 1, 2, \ldots n)$ = value of a risk indicator for a phase; and $w_i$ $(i = 1, 2, \ldots n)$ = weight assigned to each indicator. In this study, $w_i$ $(i = 1, 2, \ldots n)$ was set to 1 for both scoring models and $n = 15$, the total number of the risk indicators.

In both aggregation-based and multiplication scoring models, the phase with the highest score was ranked first (1). By applying these scoring models, this study generated risk scores for multi-angle-based ranking at different roof slopes, which are provided in Table 3.

Based on the values in Table 3, the multi-angle-based ranking of phases were computed at each slope, as shown in Fig. 6.

### Consistency Analysis for Scoring Model Selection

Because this study was to identify the riskier phases that might involve comparatively higher awkward rotations of knees and repetitions in any roof setting and, therefore, could potentially contribute to knee MSD, it was important to select the scoring model that would provide the most consistent rankings across the three roof slopes. For that reason, the scoring model to be used in the subsequent risk assessment was selected based on the consistency of the multi-angle-based rankings across the different roof slopes. Spearman's rank correlation test was used to analyze the association of the multi-angle-based rankings between every two slopes. This approach was used to identify which scoring model provided the maximum number of strongest associations and, hence, consistency of rankings across the different roof slopes. A coefficient close to one (1) suggests a strong association.

The results of Spearman's correlation for testing the rank association between slopes are provided in Table 4. For the left knee, the strongest association of ranks between 0° and 15° and between 0° and 30° slopes was obtained by the multiplication scoring model (0.929). Between 15° and 30° slopes, the strongest association was obtained by both multiplication and aggregation-based scoring models for which normalization was done by dividing by the maximum (0.893). For the right knee, the strongest rank association between 0° and 15° slopes was obtained by the aggregation-based model for which normalization was done by dividing by the maximum and by dividing by the sum (0.929). Between 15° and 30° slopes, the strongest associations were observed for both the multiplication and aggregation-based scoring models for which normalization was done by dividing by the maximum and dividing by the sum (0.893). Finally, between 0° and 30° slopes, only the multiplication scoring model provided the strongest rank association (0.964). Based on these results, it was concluded that the multiplication scoring model could compute the most consistent ranks among the different roof slopes, and hence, it was used for the subsequent risk analysis. For both knees, the achieved powers of the consistency analysis between different slopes ranged from 72% to 99%, which was acceptable to demonstrate an association or causal relationship between two variables (Cohen 2013).

**Table 3.** Risk scores of seven phases

| | Left knee | | | | Right knee | | | | |
|---|---|---|---|---|---|---|---|---|---|
| | | Aggregation | | | | Aggregation | | | |
| Phase | Multiplication ($\times 10^{26}$) | Divide by maximum | Range normalization | Divide by sum | Multiplication ($\times 10^{26}$) | Divide by maximum | Range normalization | Divide by sum | Slope |
| 1 | 1.70 | 10.80 | 6.60 | 2.10 | 47.00 | 11.60 | 9.50 | 2.40 | 0° |
| 2 | 56.00 | 13.00 | 8.00 | 3.00 | 1,070.00 | 13.00 | 11.00 | 3.00 | |
| 3 | 0.02 | 9.40 | 4.70 | 1.70 | 0.04 | 8.50 | 4.00 | 1.60 | |
| 4 | 0.04 | 9.00 | 3.00 | 1.60 | 1.00 | 9.50 | 5.80 | 1.80 | |
| 5 | 41.00 | 12.70 | 9.00 | 2.60 | 49.00 | 11.00 | 5.40 | 2.30 | |
| 6 | 0.80 | 11.00 | 6.65 | 2.06 | 0.30 | 8.80 | 3.50 | 1.70 | |
| 7 | 1.10 | 10.70 | 7.50 | 2.04 | 6.00 | 10.00 | 7.00 | 2.00 | |
| 1 | 2.10 | 10.40 | 7.00 | 2.05 | 170.00 | 12.00 | 10.30 | 2.50 | 15° |
| 2 | 192.00 | 13.00 | 9.50 | 3.00 | 740.00 | 13.00 | 9.80 | 2.90 | |
| 3 | 0.20 | 9.80 | 6.70 | 1.80 | 0.10 | 8.65 | 4.00 | 1.60 | |
| 4 | 0.10 | 9.00 | 4.50 | 1.70 | 0.30 | 8.70 | 3.50 | 1.65 | |
| 5 | 15.00 | 11.40 | 6.00 | 2.40 | 41.00 | 10.65 | 5.00 | 2.25 | |
| 6 | 0.60 | 10.00 | 4.60 | 2.00 | 0.50 | 9.00 | 3.00 | 1.70 | |
| 7 | 3.10 | 10.50 | 6.60 | 2.10 | 108.00 | 11.80 | 10.00 | 2.40 | |
| 1 | 5.60 | 10.70 | 7.80 | 2.10 | 57.00 | 11.50 | 10.00 | 2.30 | 30° |
| 2 | 722.00 | 13.50 | 10.00 | 3.00 | 530.00 | 12.60 | 7.60 | 3.00 | |
| 3 | 0.10 | 9.00 | 3.00 | 1.60 | 0.06 | 8.00 | 2.00 | 1.50 | |
| 4 | 3.00 | 10.40 | 6.00 | 2.00 | 1.00 | 9.00 | 3.70 | 1.80 | |
| 5 | 67.00 | 11.60 | 7.00 | 2.50 | 157.00 | 11.60 | 7.00 | 2.50 | |
| 6 | 0.20 | 9.30 | 3.50 | 1.70 | 2.00 | 10.00 | 5.40 | 1.90 | |
| 7 | 6.00 | 10.80 | 8.00 | 2.05 | 15.00 | 10.80 | 8.60 | 2.00 | |

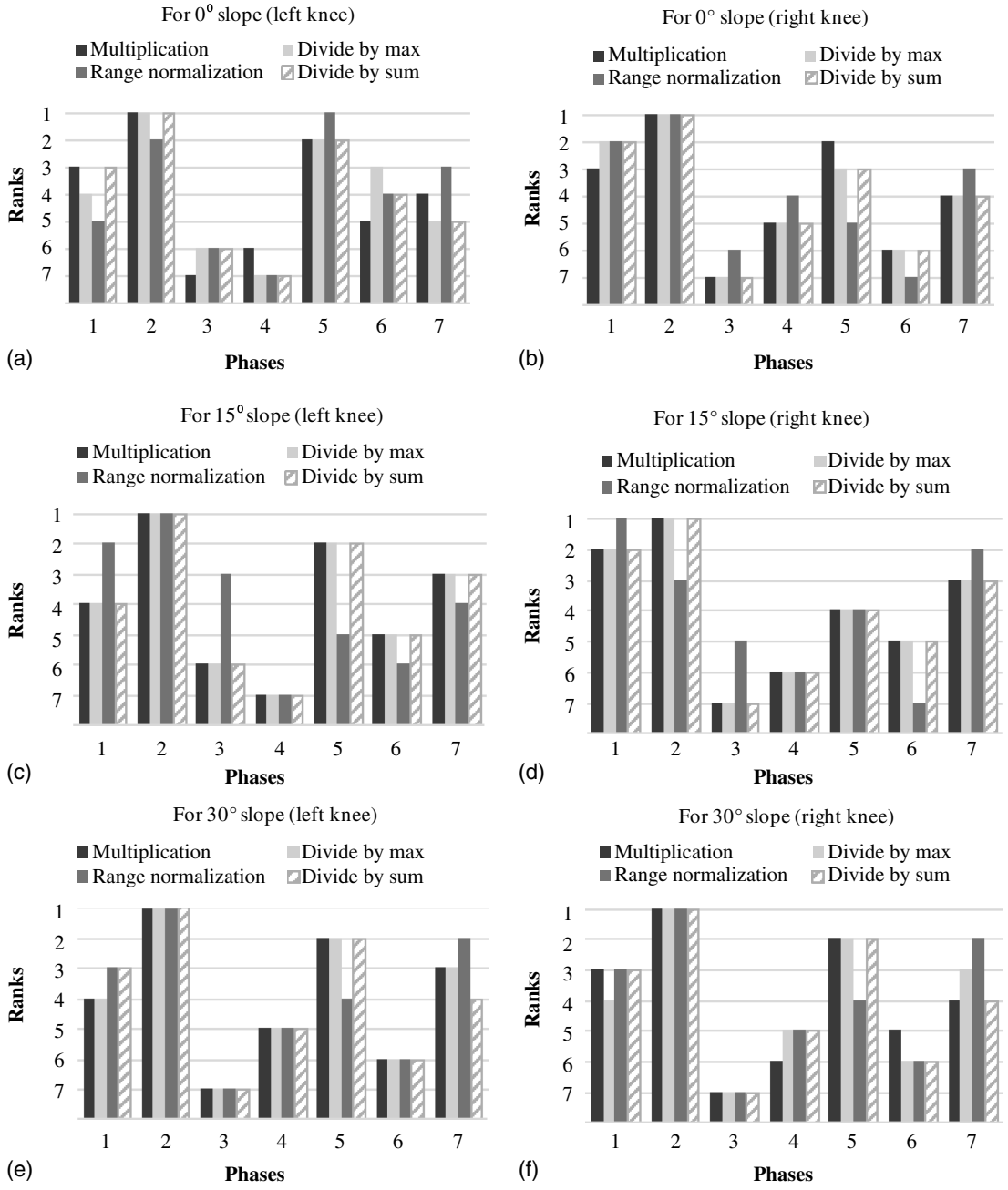


**Fig. 6.** Multi-angle-based ranks of seven phases: (a) 0° slope (left knee); (b) 0° slope (right knee); (c) 15° slope (left knee); (d) 15° slope (right knee); (e) 30° slope (left knee); and (f) 30° slope (right knee).

**Table 4.** Spearman's correlation coefficients between two slopes by different ranking models

| | Multiplication | | Divide by maximum | | Range normalization | | Divide by sum | |
|---|---|---|---|---|---|---|---|---|
| Slope | Left | Right | Left | Right | Left | Right | Left | Right |
| 0°–15° | **0.929** | 0.857 | 0.857 | **0.929** | 0.286 | 0.786 | 0.893 | **0.929** |
| 0°–30° | **0.929** | **0.964** | 0.679 | 0.929 | 0.571 | 0.714 | 0.821 | 0.929 |
| 15°–30° | **0.893** | **0.893** | **0.893** | **0.893** | 0.536 | 0.857 | 0.857 | **0.893** |

Note: Bolded numbers indicate the strongest rank association.

### Multi-Angle-Based Risks

According to the values in Table 3 and Fig. 6, for the left knee, at all three slopes, Phase 2 scored the highest, and Phase 5 scored the second highest; and thus, they were ranked first and second, respectively. The next riskiest phases were Phase 7 (ranked fourth at 0° and third at 15° and 30° slopes) and Phase 1 (ranked third at 0° and fourth at 15° and 30° slopes).

For the right knee, Phase 2 scored the highest and was ranked first at all three slopes. The next riskiest phases were Phase 5 (ranked second at 0° and 30° and fourth at 15° slopes) and Phase 1

**Table 5.** Ranks of seven phases for each knee angle

| | | Ranks | | | | | |
|---|---|---|---|---|---|---|---|
| | | Slopes (left knee) | | | Slopes (right knee) | | |
| Angle | Phases | 0° | 15° | 30° | 0° | 15° | 30° |
| Flexion | 1 | 3 | 4 | 3 | 3 | 4 | 3 |
| | 2 | 1 | 1 | 1 | 1 | 1 | 1 |
| | 3 | 7 | 7 | 7 | 7 | 7 | 7 |
| | 4 | 5 | 5 | 5 | 5 | 5 | 5 |
| | 5 | 2 | 2 | 2 | 2 | 2 | 2 |
| | 6 | 6 | 6 | 6 | 6 | 6 | 6 |
| | 7 | 4 | 3 | 4 | 4 | 3 | 4 |
| Abduction | 1 | 3 | 3 | 4 | 1 | 1 | 2 |
| | 2 | 2 | 1 | 2 | 2 | 2 | 3 |
| | 3 | 7 | 6 | 7 | 7 | 6 | 7 |
| | 4 | 6 | 7 | 3 | 5 | 7 | 6 |
| | 5 | 4 | 2 | 1 | 4 | 4 | 4 |
| | 6 | 5 | 5 | 6 | 6 | 5 | 5 |
| | 7 | 1 | 4 | 5 | 3 | 3 | 1 |
| Adduction | 1 | 4 | 5 | 3 | 5 | 4 | 3 |
| | 2 | 2 | 3 | 1 | 1 | 1 | 1 |
| | 3 | 6 | 6 | 7 | 4 | 7 | 7 |
| | 4 | 7 | 7 | 5 | 3 | 5 | 5 |
| | 5 | 1 | 1 | 4 | 2 | 2 | 2 |
| | 6 | 3 | 2 | 6 | 6 | 6 | 6 |
| | 7 | 5 | 4 | 2 | 7 | 3 | 4 |
| Internal rotation | 1 | 4 | 2 | 2 | 3 | 3 | 3 |
| | 2 | 2 | 1 | 1 | 1 | 1 | 1 |
| | 3 | 6 | 6 | 6 | 7 | 6 | 6 |
| | 4 | 7 | 4 | 5 | 4 | 5 | 5 |
| | 5 | 1 | 5 | 4 | 2 | 4 | 2 |
| | 6 | 3 | 7 | 7 | 6 | 7 | 7 |
| | 7 | 5 | 3 | 3 | 5 | 2 | 4 |
| External rotation | 1 | 3 | 5 | 7 | 1 | 1 | 3 |
| | 2 | 2 | 1 | 1 | 4 | 3 | 4 |
| | 3 | 7 | 3 | 6 | 7 | 7 | 7 |
| | 4 | 5 | 4 | 3 | 6 | 6 | 6 |
| | 5 | 1 | 2 | 2 | 3 | 4 | 1 |
| | 6 | 6 | 7 | 4 | 5 | 5 | 2 |
| | 7 | 4 | 6 | 5 | 2 | 2 | 5 |

(ranked second at 15° and third at 0° and 30° slopes). The least risky phases for both knees were Phases 4, 6, and 3.

### Single-Angle-Based Rankings by the Multiplication Scoring Model

Table 5 shows the phase rankings for each knee angle. The resulting single-angle-based rankings demonstrated a certain pattern of risk at the seven phases across three slopes but not quite consistently. Therefore, averaging the ranks across the three slopes was performed, and the results are presented in Table 6. From Table 6, it is evident that Phase 2 involved the highest flexion, abduction, adduction, and internal and external rotations for the left knee at all three roof slopes and, hence, could be deemed as the riskiest phase in terms of awkward knee rotations during sloped shingle installation. As to flexion, abduction, and external rotation, the next riskiest phase was Phase 5, when the participants faced extreme adduction as well. According to the ranking results, the next riskiest phases were Phases 1 and 7, because Phase 1 was ranked third in terms of flexion, abduction, and adduction; and Phase 7 was ranked fourth in terms of flexion, and internal and external rotations, second in terms of adduction, and third in terms of abduction. Similarly, for the right knee, at Phase 2, the participants experienced the highest amount of flexion, adduction, and internal rotation, which turned out to be riskiest. The next riskiest phases were Phases 1 and 5. Phase 1 generated the highest amount of abduction and external rotation, and Phase 5 was ranked second in terms of flexion, adduction, and internal and external rotations. After Phases 2, 5, and 1, the next riskiest phase for the right knee was Phase 7 that was ranked second in terms of abduction and third in terms of external rotation. The ranking results revealed that, in terms of awkward knee rotations, Phases 4, 6, and 3 were the least risky phases for both knees.

### Spearman's Correlation Test Result to Assess Relative Contributions of Each Angle

Table 7 presents the level of association between the multi-angle- and single-angle-based rankings at each slope. For the left knee, the flexion-based ranking was most significantly associated with the multi-angle-based rankings at the 0° and 30° slopes ($r = 0.964$, $p$ value $= 0.003$), whereas the abduction-based ranking was most significantly associated with the 15° slope ($r = 0.964$, $p$ value $= 0.003$). For the right knee, the flexion-based ranking was most significantly associated with the multi-angle-based ranking at the 0° slope ($r = 1$, $p$ value $= 0.000$). At the 15° slope, the abduction-based ranking ($r = 0.929$, $p$ value $= 0.007$) and at the 30° slope, both the flexion- and adduction-based rankings were most significantly associated with the multi-angle-based ranking ($r = 0.964$, $p$ value $= 0.003$). These results implied that, flexion, abduction, and adduction most significantly contributed to the MSD risk measurement.

## Discussion

The goal of this study was to apply ranking methods to a shingle installing process to determine if the methods could provide useful risk rankings for potential knee MSD. Fifteen risk indicators of

**Table 6.** Averaged single-angle-based phase ranks over three slopes

| | Phases | | | | | | | | | |
|---|---|---|---|---|---|---|---|---|---|---|
| | Left | | | | | Right | | | | |
| Rank | Flexion | Abduction | Adduction | Internal rotation | External rotation | Flexion | Abduction | Adduction | Internal rotation | External rotation |
| 1 | 2 | 2 | 2, 5 | 2 | 2 | 2 | 1 | 2 | 2 | 1 |
| 2 | 5 | 5 | 6, 7 | 1 | 5 | 5 | 2, 7 | 5 | 5 | 5 |
| 3 | 1 | 1, 7 | 1 | 5 | 4 | 1 | 5 | 1 | 1 | 7 |
| 4 | 7 | 4, 6 | 3, 4 | 7 | 1, 7 | 7 | 6 | 4 | 7 | 2 |
| 5 | 4 | 3 | | 4 | 3 | 4 | 4 | 7 | 4 | 6 |
| 6 | 6 | | | 6 | 6 | 6 | 3 | 6, 3 | 3 | 4 |
| 7 | 3 | | | 3 | | 3 | | | 6 | 3 |

**Table 7.** Level of association between multi-angle- and single-angle-based phase ranks

| Angle | Spearman correlation ($r$) | $p$ value | Slope (°) | Knee |
|---|---|---|---|---|
| Flexion | 0.964[a] | 0.003[a] | 0° | Left |
| Abduction | 0.75 | 0.750 | | |
| Adduction | 0.821 | 0.034 | | |
| Internal rotation | 0.821 | 0.034 | | |
| External rotation | 0.929 | 0.007 | | |
| Flexion | 0.893 | 0.012 | 15° | |
| Abduction | 0.964[a] | 0.003[a] | | |
| Adduction | 0.714 | 0.088 | | |
| Internal rotation | 0.536 | 0.236 | | |
| External rotation | 0.429 | 0.354 | | |
| Flexion | 0.964[a] | 0.003[a] | 30° | |
| Abduction | 0.821 | 0.034 | | |
| Adduction | 0.893 | 0.012 | | |
| Internal rotation | 0.821 | 0.034 | | |
| External rotation | 0.607 | 0.167 | | |
| Flexion | 1.00[a] | 0.000[a] | 0° | Right |
| Abduction | 0.821 | 0.034 | | |
| Adduction | 0.536 | 0.234 | | |
| Internal rotation | 0.964 | 0.003 | | |
| External rotation | 0.643 | 0.139 | | |
| Flexion | 0.821 | 0.034 | 15° | |
| Abduction | 0.929[a] | 0.007[a] | | |
| Adduction | 0.821 | 0.034 | | |
| Internal rotation | 0.857 | 0.023 | | |
| External rotation | 0.893 | 0.012 | | |
| Flexion | 0.964[a] | 0.003[a] | 30° | |
| Abduction | 0.679 | 0.109 | | |
| Adduction | 0.964[a] | 0.003[a] | | |
| Internal rotation | 0.893 | 0.012 | | |
| External rotation | 0.643 | 0.138 | | |

[a]Most significant $r$ and $p$ values.

knee MSD associated with awkward knee rotational angles were combined by using a scoring model to generate risk scores of the phases that led to a ranking of the phases.

Of the two scoring models explored in this study for ranking, the aggregation-based scoring model showed some inconsistencies in ranking depending on the selection of the normalization process. The multiplication scoring model generally overcame this kind of inconsistency, because this model does not need normalization. For data sets in which indicators have different numerical scales, the multiplication scoring model presents better performance, grounded that rescaling of any particular indicator generates no impacts on the ranking outcome in this model (Tofallis 2012). Among the three metrics considered in this study, the cumulative angle values were much greater than the maximum and average angle values. The multiplication scoring model thus minimized the chances of cumulative angles, even without normalization, influencing the ranks. To assure the consistencies of ranks across different roof slopes, Spearman's rank correlation test was used. The result showed that the multiplication scoring model was more consistent in generating ranks across different roof slopes and, hence, was found more suitable for this study. At all three roof slopes, though, the measured individual knee rotation angles varied, the ranking results presented similar risk patterns. The variation in individual knee rotations due to slope change could slightly change the resulting risk scores of the phases, but it did not influence their overall risk pattern across different slopes. In other words, the comparative risks among the phases were not substantially affected across different slopes. Nevertheless, this observation should be further confirmed.

Based on awkward knee rotations, the multi-angle-based ranking suggested that both knees were exposed to the greatest potential knee MSD risk while placing shingles (Phase 2). The next suggested riskiest phase was while nailing shingles (Phase 5). One possible reason for this result might be that these two phases of shingle installation operation require more repetition of extreme and awkward movement of the knees than other phases. In these phases, the participants encountered larger awkward knee rotations, multiple times, while leaning forward to grasp the shingles and while moving backward for placing and nailing them. These repetitive motions, along with awkward rotations, might lead to extra stress and force sustained by the knee joint ligaments; these operations turned out to be potentially risky phases for knee MSD. Another reason could be that the duration of these two phases were also relatively longer, which contributed to the higher cumulative awkward knee rotations for extended periods of time. In this study, the risk scores computed by using the scoring model took into account the maximum, cumulative, and average of the knee rotation angles (risk indicators in this study), which represented the risk of extreme knee rotation due to forceful exertion and prolonged and repeated awkward kneeling, respectively—the knee MSD risk factors. As these two phases involved more repetition of extreme and awkward knee rotations for a longer duration than other phases, the risk scores were also probably higher in these two phases.

On average, the single-angle-based rankings demonstrated a risk pattern similar to the multi-angle-based ranking. Among all seven phases, the placing shingle (Phase 2) and the nailing shingle (Phase 5) phases were found to be the potentially riskiest phases with extreme awkward knee rotations. The ranking results demonstrated that these two phases were ranked either first or second for a majority of the individual knee rotation angles. For example, for the left knee, all five knee rotations, and for the right knee, flexion, adduction, and internal rotations, were extreme in Phase 2. Although during the reaching for shingles phase (Phase 1), the subjects seemed to experience extreme abduction and external rotation in the right knee (ranked first for abduction and external rotation in right knee); overall, the awkward knee rotations imposed by all other lower-ranked phases were less extreme than that imposed by the placing and the nailing shingles phases. One possible reason could be the higher postural sway required during placing and nailing shingles on sloped rooftops. Subjects needed to maintain their balance on the inclined roof surface by raising their bodies' center of mass, which might force their knees to rotate more awkwardly and repeatedly, sometimes more than the normal tolerance limit. In all other phases, the participants either leaned forward to reach for shingles and moved backward to return to the resting position or used their nailing hand to grab and replace the nail gun. These phases required very few rotation movements in the knees and, hence, imposed less postural awkwardness.

Spearman's correlation test results to assess the relative contributions of each knee angle demonstrated that, for the left knee, flexion and abduction, and for the right knee, flexion, abduction, and adduction, significantly contributed to the potential knee MSD risk measurement. However, further biomechanical studies are needed to investigate the impacts of these knee rotations on knee MSD. To the best of the authors' knowledge, so far, no publications available have measured the knee MSD risk by exploiting the relative contribution of the knee rotation angles. This finding can be used as a guide in identifying which knee rotations might be prioritized for developing knee MSD risk assessment tools and effective interventions to prevent knee injuries among roofers.

Based on this discussion, it is evident that special considerations, such as knee interventions and protective measures, are essential so that knee flexion, abduction, and adduction can be

minimized during awkward kneeling while placing and nailing shingles on slanted roof surfaces. Possible interventions include wearing knee-protecting devices, such as knee pads or knee savers while kneeling, which can minimize the impact on knees. However, these interventions were not tested in this study. Because the goal was to suggest the risky phases in terms of awkward knee rotation, this study did not use any interventions (wearable or external), because they could have altered knee rotations. Also, participants were not professional roofers, and there might be some postural variations between professional and nonprofessional roofers based on their working techniques, which might impact knee rotations. Hence, further biomechanical assessment is needed to understand those variations in knee kinematics between professional and nonprofessional roofers, and the impact of knee-protecting devices needs assessment as well.

This study used nine participants' knee kinematics data to compute risk indicators. Typically, the relationship between kinematics (i.e., knee rotational angles) and musculoskeletal loadings, which is associated with MSD, is influenced by biomechanics. This relationship warranted the sample size of nine subjects appropriate for this study, and a large sample size was not necessary. In the research community, it is well accepted to use fewer than ten subjects for risk analysis with biomechanical models.

### *Study Limitations*

First, the experiment was completed in a controlled laboratory setting rather than on a construction site to minimize possible risk of injury to participants. Although the experiment was designed based on common site practices and the participants simulated the shingle installation task to capture a real scenario of a construction site, further assessment in a real work setting is still needed to justify the findings. Second, none of the study participants were experienced roofers. However, they were physically active and had working experience with home remodeling projects. From a biomechanical perspective, there should be some difference between novice and experienced roofers, but in this study novice roofers were chosen to identify the risk that an individual without any prior roofing experience may face when that individual first gets exposed to a slanted roof top during shingle installation. This study presumed considerably similar biomechanical reactions of the participants and professional roofers. However, if professional roofers were used, it could have altered the individual knee rotations to some extent. Therefore, further assessment is necessary to justify such premise. The goal of this study was to identify an ergonomic method for suggesting the risky phases in the shingle installation process, and the subject tests only served to demonstrate the procedure and the framework. Third, this study only focused on risks to knee MSD, excluding associated risks to other lower extremities, such as ankles, that may undergo excessive pressure during shingle installation. Finally, this study identified risky phases only based on knee rotations. Other indicators (e.g., muscle activations and joint loadings) for knee MSD risks would be complementary but were not assessed in this study.

## Conclusion and Future Extension

This study identified an ergonomic method for ranking the relative risks of the shingle installation phases to knee MSD development. The results suggested that the phases of placing and nailing shingles are the riskiest phases in terms of awkward rotation and repetition; and the awkward flexion, abduction, and adduction can potentially contribute the most to knee injury risk measurement.

All the findings have been drawn from the experimental study done with nonprofessional roofers and, hence, might not be generalizable. Future work will include professional roofers to study knee MSD risk in shingle installation, including starter and ridge cap shingles. Moreover, effective knee interventions (wearable and external) will be tested and developed with their participation in real work settings. Electromyography signals of thigh muscles and knee joint loadings will be observed and analyzed. This study provided a method that may generate useful information about the unsafe condition of shingle installation operations to facilitate effective intervention strategies (education, training, and tools) for reducing knee exposure and, hence, minimize knee injuries and disorders among construction roofers.

## Data Availability Statement

Data generated or analyzed during the study are available from the corresponding author by request. Information about the *Journal*'s data-sharing policy can be found here: http://ascelibrary.org/doi/10.1061/(ASCE)CO.1943-7862.0001263.

## Acknowledgments

The authors acknowledge the support of the National Institute for Occupational Safety and Health, who funded this research. The findings and conclusions in this research are those of the authors and do not necessarily represent the opinion of the National Institute for Occupational Safety and Health, Centers for Disease Control and Prevention.

## References

Albers, J., and C. F. Estill. 2007. *Simple solutions: Ergonomics for construction workers*. Cincinnati: National Institute for Occupational Safety and Health.

Bagaya, O., and J. Song. 2016. "Empirical study of factors influencing schedule delays of public construction projects in Burkina Faso." *J. Manage. Eng.* 32 (5): 05016014. https://doi.org/10.1061/(ASCE)ME.1943-5479.0000443.

Barrios, J. A., K. M. Crossley, and I. S. Davis. 2010. "Gait retraining to reduce the knee adduction moment through real-time visual feedback of dynamic knee alignment." *J. Biomech.* 43 (11): 2208–2213. https://doi.org/10.1016/j.jbiomech.2010.03.040.

BLS (US Bureau of Labor Statistics). 2017. "Nonfatal cccupational injuries and illnesses: Cases with days away from work." Accessed March 4, 2019. https://www.bls.gov/news.release/pdf/osh2.pdf.

Breloff, S. P., A. Dutta, F. Dai, E. W. Sinsel, C. M. Warren, X. Ning, and J. Z. Wu. 2019a. "Assessing work-related risk factors for musculoskeletal knee disorders in construction roofing tasks." *Appl. Ergon.* 81 (Nov): 102901. https://doi.org/10.1016/j.apergo.2019.102901.

Breloff, S. P., C. Wade, and D. E. Waddell. 2019b. "Lower extremity kinematics of cross-slope roof walking." *Appl. Ergon.* 75 (Feb): 134–142. https://doi.org/10.1016/j.apergo.2018.09.013.

Choi, S. D. 2008. "Postural balance and adaptations in transitioning sloped surfaces." *Int. J. Constr. Educ. Res.* 4 (3): 189–199. https://doi.org/10.1080/15578770802494581.

Cohen, J. 2013. *Statistical power analysis for the behavioral sciences*. New York: Lawrence Erlbaum Associates.

Coplan, J. A. 1989. "Rotational motion of the knee: A comparison of normal and pronating subjects." *J. Orthopaedic Sports Physical Ther.* 10 (9): 366–369. https://doi.org/10.2519/jospt.1989.10.9.366.

CPWR (Center for Construction Research and Training). 2018. *The construction chart book : The United States construction industry and its workers*. 6th ed. Silver Spring, MD: CPWR.

Dulay, G. S., C. Cooper, and E. Dennison. 2015. "Knee pain, knee injury, knee osteoarthritis & work." *Best Pract. Res. Clin. Rheumatol.* 29 (3): 454–461. https://doi.org/10.1016/j.berh.2015.05.005.

El-Sayegh, S. M., and M. H. Mansour. 2015. "Risk assessment and allocation in highway construction projects in the UAE." *J. Manage. Eng.* 31 (6): 04015004. https://doi.org/10.1061/(ASCE)ME.1943-5479.0000365.

Fredericks, T. K., O. Abudayyeh, S. D. Choi, M. Wiersma, and M. Charles. 2005. "Occupational injuries and fatalities in the roofing contracting industry." *J. Constr. Eng. Manage.* 131 (11): 1233–1240. https://doi.org/10.1061/(ASCE)0733-9364(2005)131:11(1233).

Gyemi, D. L., P. M. van Wyk, M. Statham, J. Casey, and D. M. Andrews. 2016. "3D peak and cumulative low back and shoulder loads and postures during greenhouse pepper harvesting using a video-based approach." *Work* 55 (4): 817–829. https://doi.org/10.3233/WOR-162442.

Hatfield, G. L., W. D. Stanish, and C. L. Hubley-Kozey. 2015. "Three-dimensional biomechanical gait characteristics at baseline are associated with progression to total knee arthroplasty." *Arthritis Care Res.* 67 (7): 1004–1014. https://doi.org/10.1002/acr.22564.

Hofer, J. K., R. Gejo, M. H. McGarry, and T. Q. Lee. 2011. "Effects on tibiofemoral biomechanics from kneeling." *Clin. Biomech.* 26 (6): 605–611. https://doi.org/10.1016/j.clinbiomech.2011.01.016.

Kajaks, T., and P. Costigan. 2015. "The effect of sustained static kneeling on kinetic and kinematic knee joint gait parameters." *Appl. Ergon.* 46 (Jan): 224–230. https://doi.org/10.1016/j.apergo.2014.08.011.

Lee, W., K.-Y. Lin, E. Seto, and G. C. Migliaccio. 2017. "Wearable sensors for monitoring on-duty and off-duty worker physiological status and activities in construction." *Autom. Constr.* 83 (Nov): 341–353. https://doi.org/10.1016/j.autcon.2017.06.012.

McClellan, A. J., W. J. Albert, S. L. Fischer, F. A. Seaman, and J. P. Callaghan. 2009. "Shoulder loading while performing automotive parts assembly tasks: A field study." *Occup. Ergon.* 8 (2): 81–90. https://doi.org/10.3233/OER-2009-0162.

Nagura, T., C. O. Dyrby, E. J. Alexander, and T. P. Andriacchi. 2002. "Mechanical loads at the knee joint during deep flexion." *J. Orthopaedic Res.* 20 (4): 881–886. https://doi.org/10.1016/S0736-0266(01)00178-4.

Nagura, T., H. Matsumoto, Y. Kiriyama, A. Chaudhari, and T. P. Andriacchi. 2006. "Tibiofemoral joint contact force in deep knee flexion and its consideration in knee osteoarthritis and joint replacement." *J. Appl. Biomech.* 22 (4): 305–313. https://doi.org/10.1123/jab.22.4.305.

OSHA (Occupational Safety and Health Administration). 2019. "Ergonomics." Accessed July 8, 2019. https://www.osha.gov/SLTC/ergonomics/training.html.

Qin, X., Y. Mo, and L. Jing. 2016. "Risk perceptions of the life-cycle of green buildings in China." *J. Cleaner Prod.* 126 (Apr): 148–158. https://doi.org/10.1016/j.jclepro.2016.03.103.

Robertson, G., G. Caldwell, J. Hamill, G. Kamen, and S. Whittlesey. 2013. *Research methods in biomechanics*, 2nd ed. Champaign, IL: Human Kinetics.

Rosso, R. 1997. *Statistics, probability and reliability for civil and environmental engineers*. New York: McGraw-Hill.

Spielholz, P., G. Davis, and J. Griffith. 2006. "Physical risk factors and controls for musculoskeletal disorders in construction trades." *J. Constr. Eng. Manage.* 132 (10): 1059–1068. https://doi.org/10.1061/(ASCE)0733-9364(2006)132:10(1059).

Thambyah, A., J. C. Goh, and S. D. De. 2005. "Contact stresses in the knee joint in deep flexion." *Med. Eng. Phys.* 27 (4): 329–335. https://doi.org/10.1016/j.medengphy.2004.09.002.

Tofallis, C. 2012. "A different approach to university rankings." *Higher Educ.* 63 (1): 1–18. https://doi.org/10.1007/s10734-011-9417-z.

Tofallis, C. 2014. "Add or multiply? A tutorial on ranking and choosing with multiple criteria." *Informs Trans. Educ.* 14 (3): 109–119. https://doi.org/10.1287/ited.2013.0124.

Wang, D., F. Dai, and X. Ning. 2015. "Risk assessment of work-related musculoskeletal disorders in construction: State-of-the-art review." *J. Constr. Eng. Manage.* 141 (6): 04015008. https://doi.org/10.1061/(ASCE)CO.1943-7862.0000979.

Wang, D., F. Dai, X. Ning, R. G. Dong, and J. Z. Wu. 2017. "Assessing work-related risk factors on low back disorders among roofing workers." *J. Constr. Eng. Manage.* 143 (7): 04017026. https://doi.org/10.1061/(ASCE)CO.1943-7862.0001320.

Washington State Department of Labor & Industries. 2018. "Rates for worker's compensation: 2018 Base rates by business type and classification code." Accessed July 10, 2019. http://www.lni.wa.gov/ClaimsIns/Files/Rates/2018RatesBusTypeClassCode.pdf.

Welch, L. S., E. Haile, L. I. Boden, and K. L. Hunting. 2010. "Impact of musculoskeletal and medical conditions on disability retirement: A longitudinal study among construction roofers." *Am. J. Ind. Med.* 53 (6): 552–560. https://doi.org/10.1002/ajim.20794.

Zampporri, J. A., and A. Aguinaldo. 2017. "The effects of compression tights on dynamic knee motion during a drop vertical jump in female college athletes." *ISBS Proc. Arch.* 35 (1): 243.